To the Graduate Council:

I am submitting herewith a thesis written by Eric James Jacob entitled "Forced Resonant Periodic Shock Waves and Mean Pressure Shift in a Closed Tube." I have examined the final electronic copy of this dissertation for form and content and recommend that it be accepted in partial fulfillment of the requirements for the degree of Masters of Science, with a major in Aerospace Engineering.

Gary Flandro
Major Professor

We have read this thesis
and recommend its acceptance:

John Steinhoff

Trevor Moeller

Accepted for the Council:

Anne Mayhew
Vice Chancellor and
Dean of Graduate Studies

(Original signatures are on file with official student records.)

Forced Resonant Periodic Shock Waves and Mean Pressure Shift in a Closed Tube

A Thesis

Presented for the

Master of Science

Degree

University of Tennessee, Knoxville

Eric James Jacob

December 2006

Acknowledgements

I would like to express a sincere ‘thank you’ to my parents, Kenneth and Kim Jacob. They have granted me every possible opportunity to excel, unconditionally. Devoid of their love and support, this stepping stone in my journey could not have come to completion. I would also like to thank Dr. Flandro. His endless knowledge of Combustion Instability and Non-Linear phenomenon has resonated in this work, and his selfless dedication to teaching and research has inspired me. As my advisor he has helped me every step of the way, offering new insights and suggestions on what to try next. He has repeatedly offered me opportunities to participate in exciting side projects that have only deepened my knowledge, abilities and passion for engineering and science. I would like to thank Dr. Moeller and Dr. Steinhoff for participating on my committee and for their valuable editorial and contextual comments. I would also like to thank several of the other graduate research assistants here at UTSI: Sean Fischbach, Mark Olles, Daniel Banuti and Joshua Batterson, for helping me when I needed an extra hand. Last of all I would like to thank God, for through him all things are possible.

Abstract

The thesis outlines an experiment done in the oscillation of a closed tube near to its fundamental frequency. A tube with a length of ten feet was oscillated via a piston driven by a DC motor. The pressure waveform and mean pressure was recorded at the end of the tube and the mean pressure was measured at the middle of the tube. When the tube was excited near to its 1st mode non-linear features such as shock-like waveforms, cascading of energy to higher modes and mean pressure shift were recorded.

These Results are only possible to predict by using a non-linear analytical approach. Work by Chester[5] successfully predicts the shock-like waveform phenomenon; however, it fails to predict the mean pressure shifts. Flandro[6,16-17] successfully correlates the shock-like waveforms and mean pressure shift in his non-linear combustion instability research.

Predicting these phenomena has critical importance to the field of combustion instability and rocket combustion chamber design. Solid and liquid rocket engines often have large amplitude pressure oscillations marked by shock-like features and mean pressure shifts. These both act to cause large mechanical vibrations, thrust variations, internal damage and catastrophic failure of the engine. Understanding these phenomena in an analytical way is important if rocket engines are to be designed in a reliable and inexpensive way. The use of the highlighted experiment in this thesis will serve to elucidate which analytical approach is the most appropriate.

Table of Contents

List of Tables

List of Figures

1. Introduction

1.1. Motivation

Stability is the largest concern in the rocket engine design field. Stability can mean the difference in whether or not your engine will fail. Shock-like waveforms and mean pressure increases are two hazardous effects that combustion instability can have on a rocket engine. The shock-like waveforms can cause large stresses on internal components, such as injectors, and send large mechanical vibrations into entire system through the variations in chamber pressure therefore through the induced variations in thrust. A mean pressure increase in conjunction with the high amplitude shock-like waveforms threatens to cause a catastrophic failure of the liquid engine or solid motor.

1.2. Historical Examples

These shock-like formations and mean pressure shifts can be seen in many historical examples of rocket motors. The most famous of all was the F-1, the engine which the mighty Saturn V rocket rode on it way to the moon. During initial testing these engines supported large oscillations in chamber pressure. Figure 1 shows a plot of the pressure in the chamber of the F-1. Each vertical block on the plot represents 250 psi and each horizontal block represents .005 sec. High amplitude 500 Hz oscillations can be seen. Typical acoustic waves have amplitudes of 0-100 dB; the oscillations in the F-1 motor have amplitudes of approximately 227 dB, far beyond the scale of conventional acoustics. (see Appendix A.1)

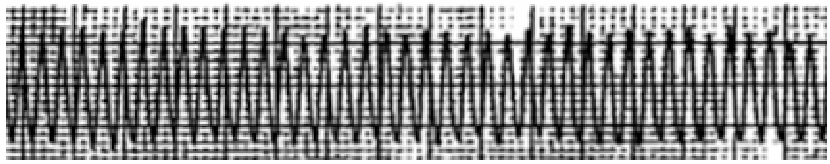

Figure 1: F-1 Pressure Recording[15]

More examples of shock-like features can be seen in Figure 2. This image shows the pressure readings from a 20,000 lbf JPL Research Motor.[7-10] The pressure sensor locations are shown in a plot beneath the pressure plots. Pulses of up to 4000 psi are present in the engine at approximately 2000 Hz, signaling the presence of shock-like steep fronted waves of the first tangential mode.

Another example of instability in rocketry can be seen in Figure 3. This figure shows the Pressure vs. Time of a solid rocket motor.[12-14] When the rocket motor is pulsed, via a small explosive charge, oscillations are provoked and large amplitude waveforms appear. These waveforms typically harmonize within the combustion chambers dimensions. A mean pressure shift, or DC shift, can be seen along with the large amplitude oscillations; showing that the two effects go hand in hand.

Many times in solid rockets, because of the changing nature of the internal dimensions of the combustion chamber due to the burning of propellant, the oscillation frequencies can change in time. Therefore, plotting the spectrum of the pressure readings vs. time in a waterfall plot can be an invaluable tool. Figure 4 shows a plot of the space shuttles solid rocket boosters (SRB) spectrum vs. time.[11] This plot shows clear signs of instability, shock-like features and vortex shedding.

The SRB spectrum waterfall shows many features which are inherent in combustion instability. Features such as the generation of harmonics are shown at 15, 30 and 45 Hz.

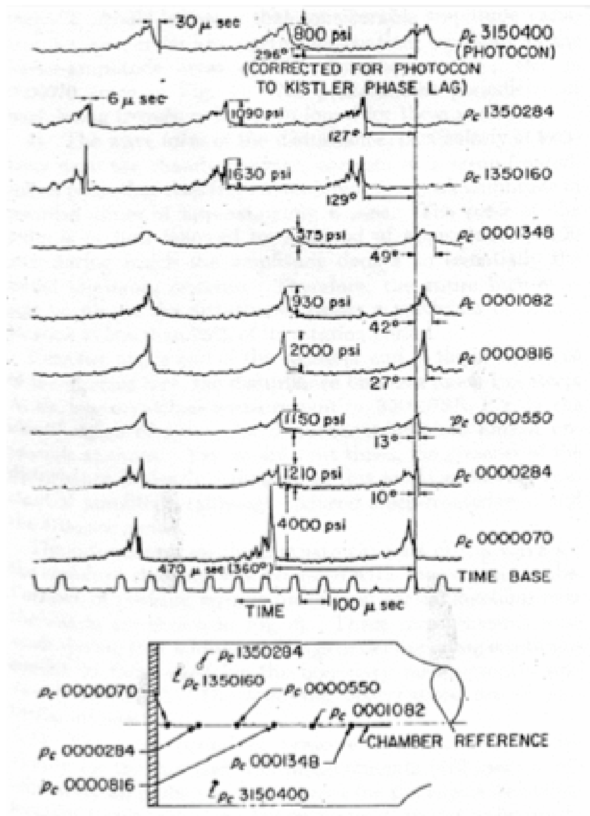

Figure 2: JPL Research Motor[7-10]

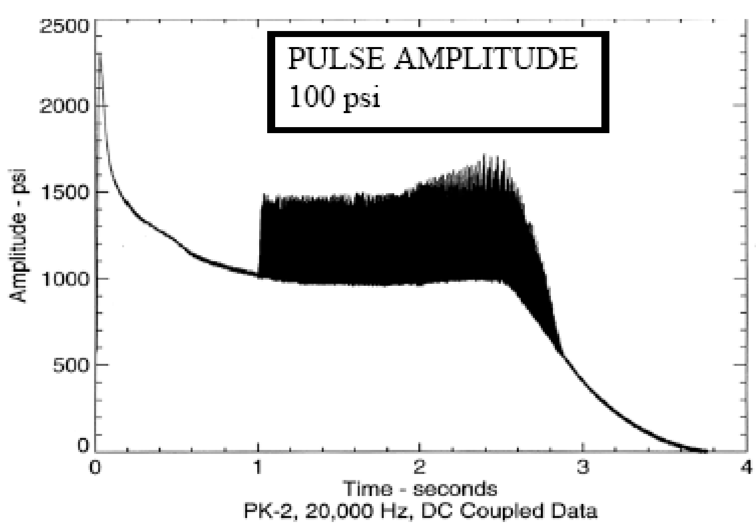

Figure 3: Oscillations in a Solid Rocket Motor[12-14]

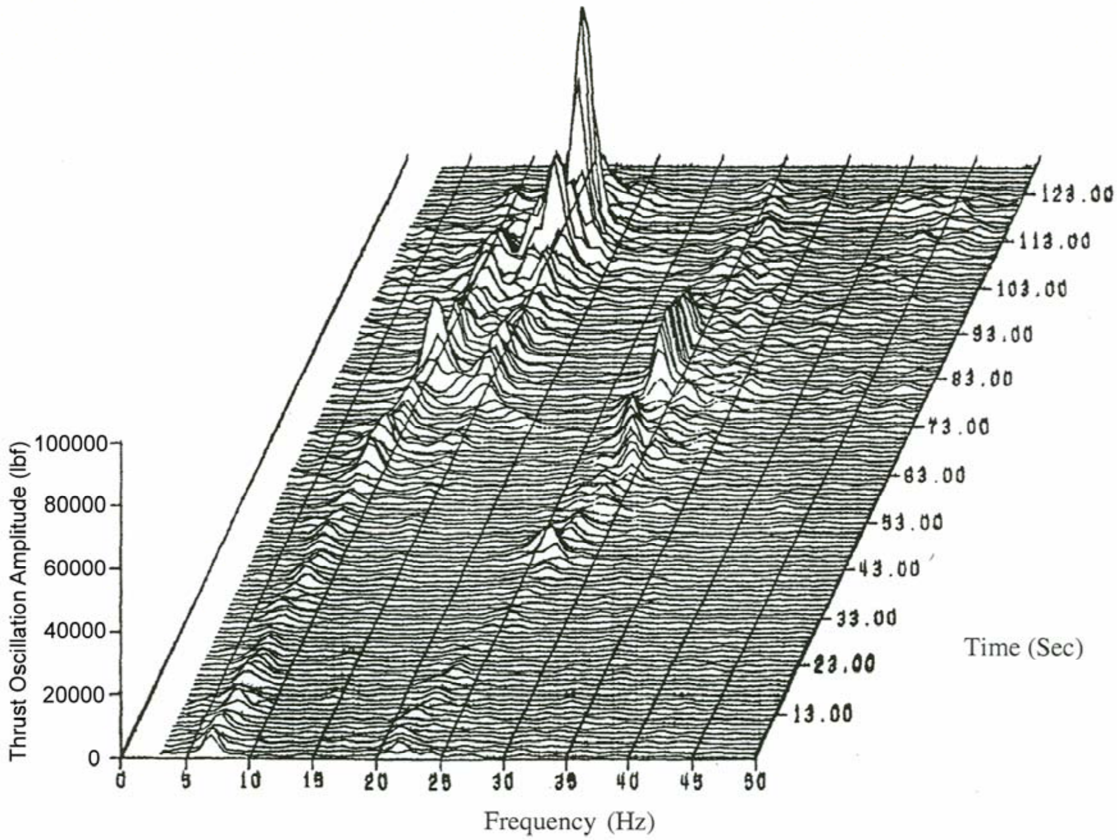

Figure 4: SRB Spectrum Waterfall[11]

Large thrust oscillations of nearly 100,000 lbf are seen at the peak amplitudes. Other effects such as vortex shedding are shown, which can be identified via the diagonal line starting at about 20 Hz and 70 sec and shifting to 15 Hz at 75 sec. These shifts can be categorized as the vortices attempting to harmonize with the natural frequencies in the combustion chamber.[11]

The source of the shock-like waveforms and mean pressure increase has been generally misunderstood. It is typically considered that these waveforms are simply the addition of separate linear acoustic modes driven independently.[18-21] The experiment which this paper highlights demonstrates, through a simple experiment, that these effects are the result of non-linear acoustics. These non-linear effects occur in a problem which is generally treated as a linear system. Neglecting the non-linear segment of the model eliminates the ability to predict key features in many unstable rockets. As it turns out, the shock-like waves and mean pressure shifts are not elements entirely related to the combustion, but rather to the non-linear acoustics that accompany resonating frequencies. The combustion instead acts much like a piston, driving the oscillations.

1.3. Saenger's Results

In 1958 Saenger[2] did a similar experiment to that reported in this thesis. His experiment consisted of a piston which was oscillated in a closed tube, with a diameter of 1.9 inches and a fundamental frequency of approximately 100 Hz. The pressure waveform and mean pressure shift where then measured at the end of the tube away from the piston. His results, shown in Figure 5, show shock-like structures and mean pressure variations similar to what is seen in the previous historical rocketry examples such as the JPL research motor (see Figure 2) and the solid rocket motor examples. (see Figure 3)

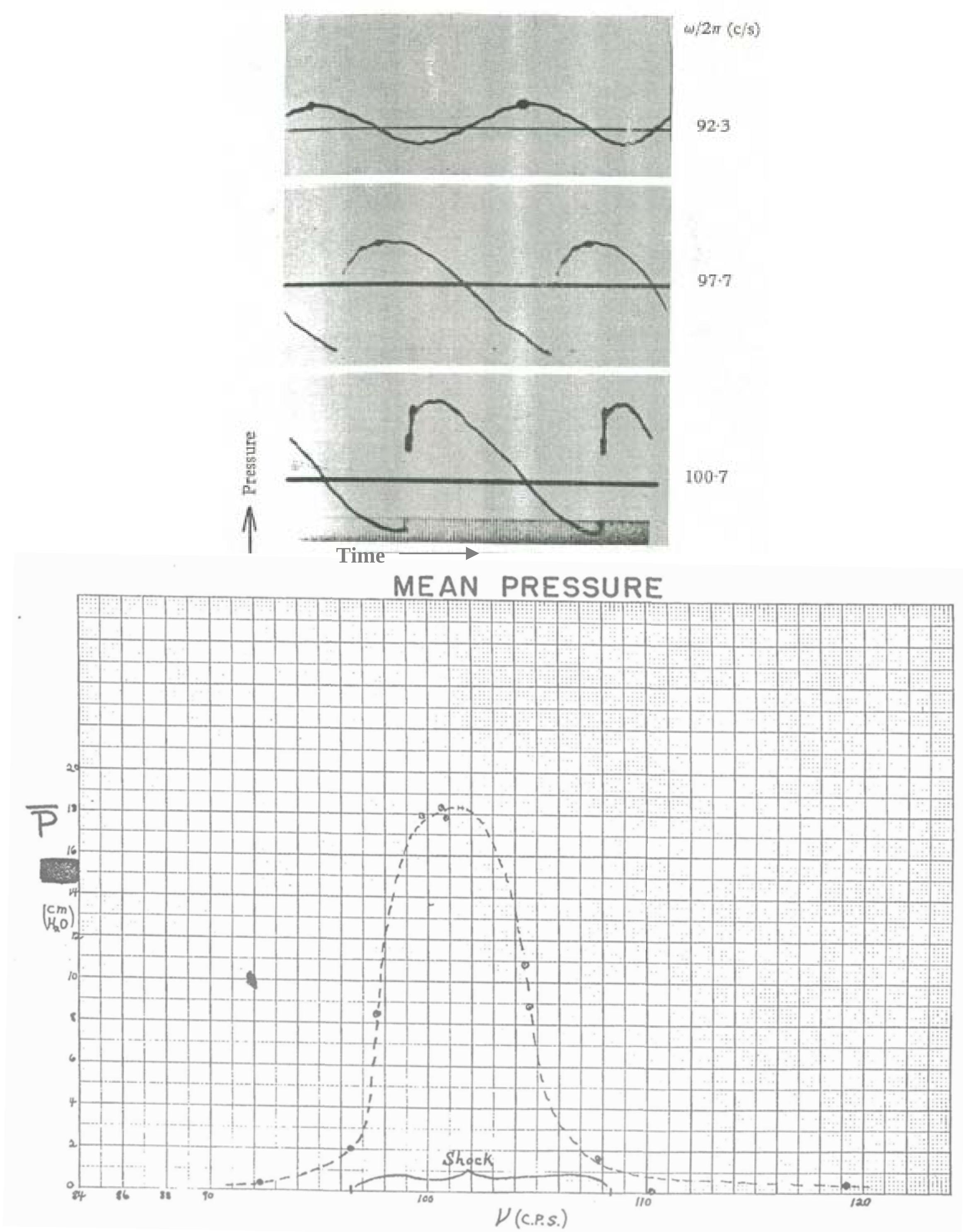

Figure 5: Saenger's Experimental Results[2]

Unfortunately, we are unable to find a full description of the dimensions of his piston, thereby making it difficult to compare to analytical work.

1.4. Chester's Results

In 1964 Chester[5] showed an analytic solution for the non-linear acoustics of a closed tube filled with gas with a piston at one end oscillating near resonance frequencies. The results of his work can be seen in Figure 6. These plots show the transition from a sinusoidal oscillation when the tube is driven away from its resonance to the shock-like structures at resonance. The value 'r' shows a relationship between the fundamental harmonic and the driving frequency. The dashed lines represent the addition of viscous boundary layer effects. Further discussion on Chester's results is located in Appendix A.6. These results show remarkable correlation to Seanger's[2] results and will be later compared to the results in the outlined experiment. However, Chester's[5] results do not account for any mean pressure increase.

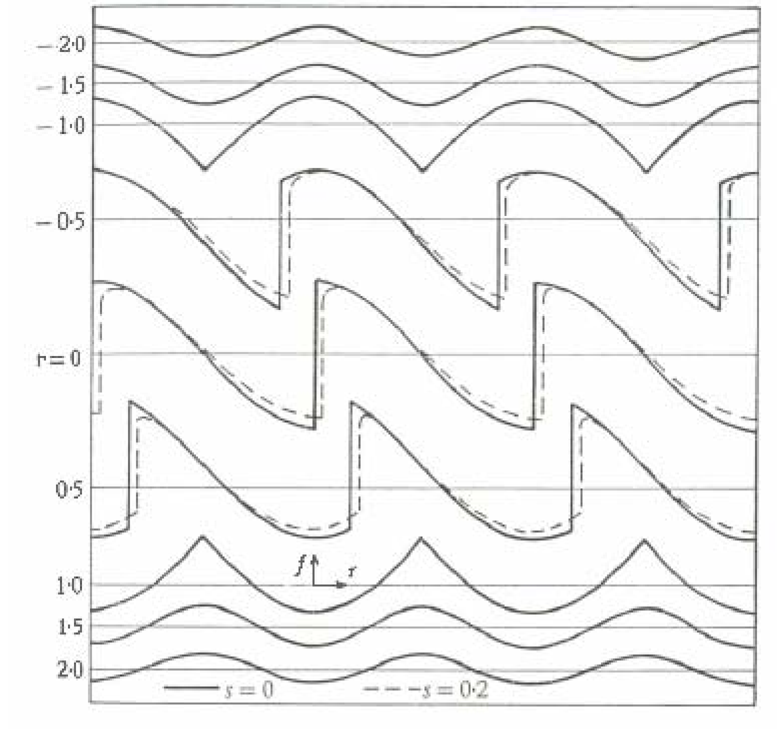

Figure 6: Chester's Analytical Results[5]

2. Experimental Setup

The experimental setup is composed of three main components: the oscillating piston, the closed tube and the pressure sensors. The oscillating piston is driven at a given frequency and the pressure fluctuations are measured by several pressure sensors. Figure 7 depicts the overall layout of the experiment.

2.1. Piston Assembly

The oscillating piston is driven by a 2500 RPM, ½ Hp DC motor connected by a ½ in. wide timing belt pulley system. The pulley setup allows a higher revolution rate at the piston yielding a maximum input frequency of 78.4 Hz, greater than the fundamental harmonic of the closed tube.

The frequency of the piston oscillation is measured in two ways. The first and more accurate way is to use a precision stroboscope to tune into the rotation of the piston crankshaft much in that same way an auto mechanic tunes a gasoline engine. This method has the advantage of being very accurate with an error of +/- .2Hz; however, it takes a significant amount of time to tune in to the correct frequency.

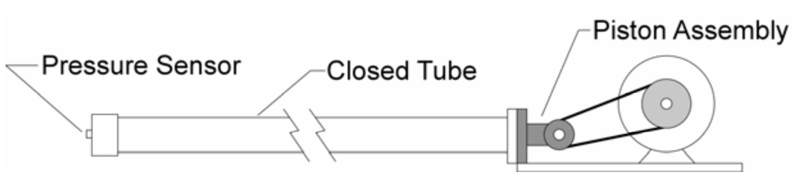

Figure 7: Experimental Setup Overview

The second and less accurate way is to use a ‘chopper wheel’ (see Fig. 8) in conjunction with an optical switch. The chopper wheel was driven on the pistons crankshaft along with the pulley as shown in Figure 9. A TDS 3054B Tektronics digital oscilloscope was used to read in the voltage output from the optical switch and automatically calculate the frequency via an internal computation option. This allowed a direct measurement of the pistons revolution rate. The optical switch when using the oscilloscopes automatic calculation had an error of +/- 1 Hz, five times larger than that associated with the precision stroboscope.

The piston is a Merco model airplane engine run in reverse, with the DC motor driving the crankshaft and oscillating the piston. All the ports entering and exiting the engine, where normally fuel, air and exhaust would flow, had to be sealed. The engine had to be regularly oiled to maintain operation because the engine did not have its normal lubricant available to it in the fuel. The piston has a stroke of 7/8 in. and a diameter of 15/16 in.

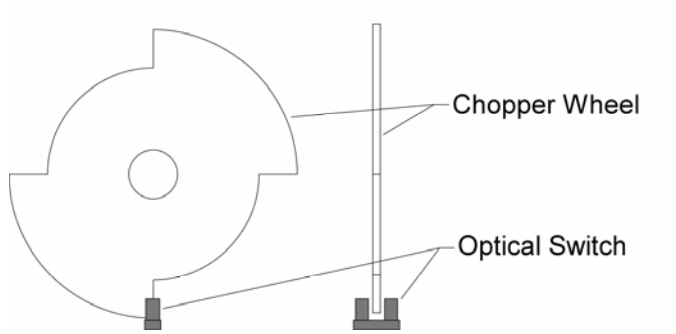

Figure 8: Optical Switch with Chopper Wheel

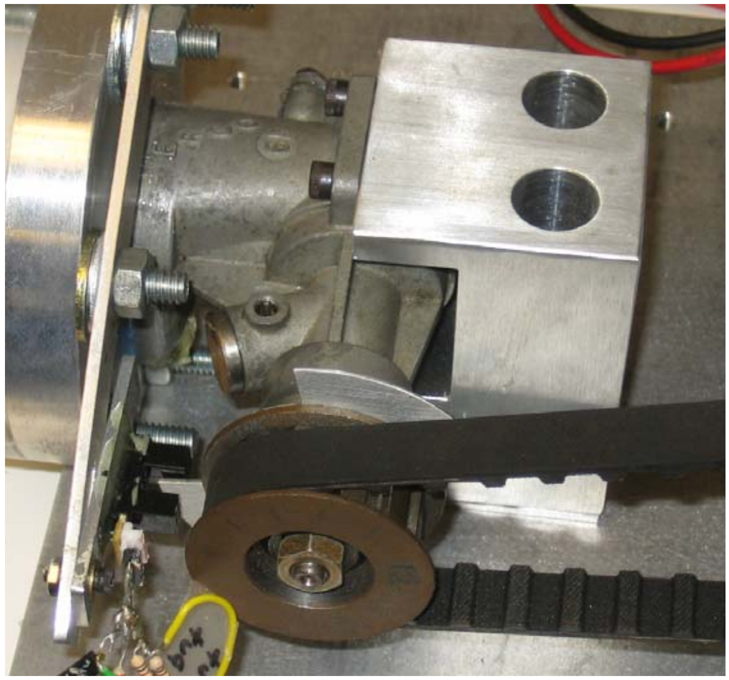

Figure 9: Piston/Chopper Wheel Connection

2.2. Closed Tube

The closed tube is made of PVC. It is 10.0 ft long (+/- .1 in) with an inside diameter of 2.0 in (+/- 1/32 in) and a wall thickness of 3/16 in (+/- 1/32 in). The PVC piping has low thermal conductivity which serves to minimize any heat flow through the tube. It also has a smooth interior surface which reduces viscous effects. The tube is capped and sealed at the end away from the piston and is securely mounted to the piston assembly. The PVC tube is held in place on the table by three clamps to minimize the mechanical vibration of the tube. The tube has a fundamental frequency, at room temperature, of approximately 56.2 Hz (+/- .5 Hz) (see Appendix A.2.)

2.3. Pressure Sensors

Three pressure sensors were employed in the experiment, one electronic pressure transducer with a range of +/- 2 psig and two water manometers. The pressure transducer was radially centered at the end of the tube away from the piston. The electronic pressure transducer had an input of 10.0 Volts (+/- .1 Volts) and an output voltage on the order of a hundred millivolts. The output voltage of the pressure sensor was linearly related to the pressure by a factor of 147.4 mV/psi.

The water manometers were located at the end of the tube, below the pressure transducer, and in the middle of the length of the tube. Figure 10 depicts the location of the pressure sensors. Having the water manometer located below the pressure transducer ensured that, in the case of an unexpected low pressure in the closed tube, any water entering the closed tube from the manometers would not harm the electronic pressure transducer.

The water manometers were hand built out of ¼ in. plastic tubing. They were fastened to the tube and held in a level manner ensuring that the pressure forces act directly against the gravitation force. A grid of 1 mm spacing was placed behind the tubes to allow measurement of the displacement of the waters height. The water manometers had an error of +/- 1 mmH2O (or +/- .00142 psi) because of the meniscus, the ability to read the scale accurately, and parallax.

The water manometers work excellently to measure the subtle increase in the mean pressure of the closed tube. The manometers have an inherent damping (because of the inertia of the water) which eliminates the oscillations induced from the piston and leaves only the DC, or steady state, pressure. However, in the future, digital manometers would be preferred due to the ease of measuring many data points compared to the manual task of measuring each water manometer.

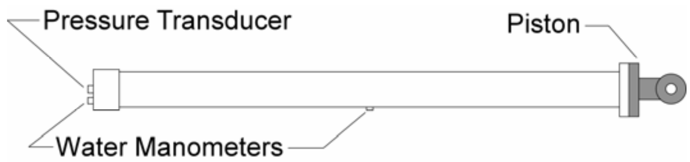

Figure 10: Location of Pressure Sensors

2.4. Pressure Seal

The system's ability to maintain pressure was tested to insure that the seals were in working order. The experiment was run shortly through its resonance point which built up the mean pressure. The piston was then stopped. The mean pressure level was watched via the water manometers. Initially one to two cmH_2O gauge of pressure was present. The pressure escaped slowly, needing nearly an hour to reduce to ambient pressure unless the pressure was released manually. This slow reduction in pressure showed that proper methods were used to seal both the tube and piston.

2.5. Measurement Procedure

The measurements were taken by an oscilloscope, the direct reading of manometers and a stroboscope. The motor was set manually to run at a given RPM. The revolution rate of the piston was then recorded with the oscilloscope/optical switch and the stroboscope.

The voltage reading from the pressure transducer and the calculated FFT spectral analysis was electronically saved off of the oscilloscope once the systems mean pressure achieved steady state. A picture was then taken of the water manometers from a set location perpendicular to the manometer and level with its zeroed state. This reduced any parallax errors. Taking the pictures allowed for a digital record of the pressure readings and also alleviated time for other tasks while the experiment was running. Once the experiment was complete the results from the oscilloscope and the pictures were loaded to a desktop PC and evaluated.

2.6. Summary of Important Experimental Attributes

A summary of significant dimensions along with their respective error is given in Table 1.

Table 1: Summary of Important Dimensions

Attribute	***Value***	***Error***
Piston Stroke	7/8 in.	+/- 1/32 in.
Piston Diameter	15/16 in.	+/- 1/32 in.
Closed Tube Length	10.0 ft	+/- 1/8 in.
Closed Tube Inside Diameter	2.0 in.	+/- 1/32 in.
Closed Tube Wall Thickness	3/16 in.	+/- 1/32 in.
Maximum Piston Frequency	78.4 Hz	N/A
Tube Fundamental Frequency [app]	56.2 Hz	+/- .3 Hz

3. Experimental Results

3.1. Fundamental Harmonic Shocking

When the closed tube was excited near its fundamental frequency it responded by producing shock-like waveforms. The amplitude of the oscillations grew quickly as the pistons frequency approached the fundamental harmonic of the tube, which is expected according to acoustic resonance theory. When the shock-like waveforms were present the tube began to mechanically vibrate slightly. The incorporation of clamps to hold down the tube reduced these vibrations significantly.

Figure 11 shows the pressure output from the transducer. This pressure was measured from the end of the tube away from the piston. The data shown in this plot was recorded at 47.72 Hz which is lower than the harmonic frequency of the tube. The oscillations are nearly sinusoidal and there is very little noise. Figure 12 shows the pressure output from the transducer taken at 56.11 Hz which is near to the harmonic frequency of the tube.

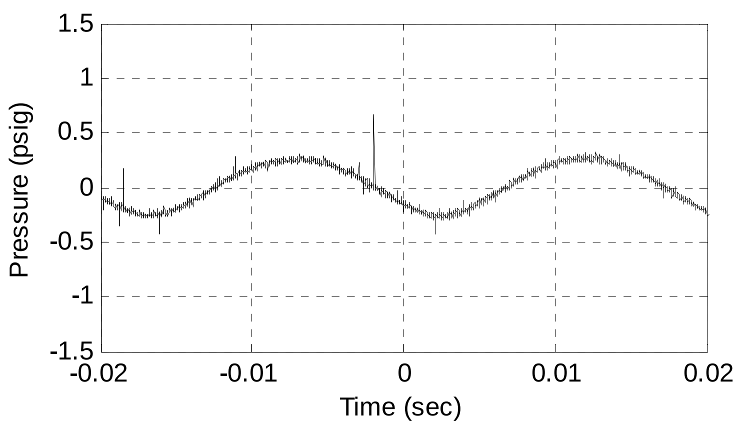

Figure 11: Pressure Measurement at 47.72 Hz

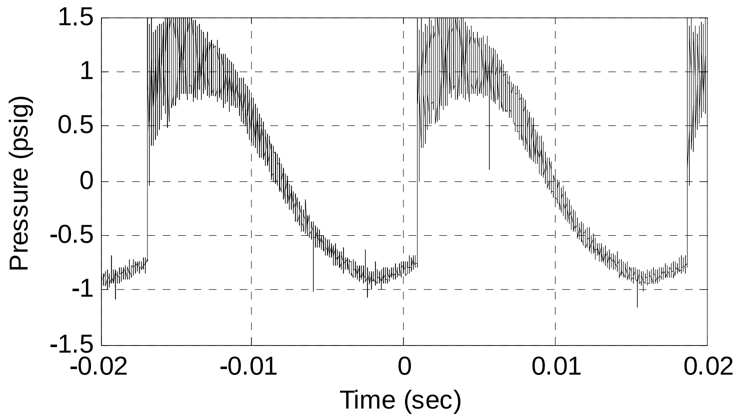

Figure 12: Pressure Measurement at 56.11 Hz

There are clear shock-like structures present in Figure 12. There is significantly more noise in the system due to the induced mechanical vibration from the piston and the violent nature of the shocks.

Figure 13 shows another measurement that was taken at 58.06 Hz, slightly higher but near to the fundamental frequency. This measurement shows the transition from the linear sinusoidal acoustics to the non-linear shock-like waveforms. Additional waveforms can be viewed in Appendix A.4.

3.2. Spectrum Analysis

At each measured input forcing frequency the pressure transducer spectrum was sampled using a built in function on the digital oscilloscope. The spectra were plotted in a waterfall plot shown in Figure 14. When the tube was excited at its fundamental frequency the shock-like waveforms were present, these shock-like formations have the characteristic of containing many harmonics. The fundamental frequency at approximately 52 Hz and the first seven harmonic frequencies are shown in Figure 14.

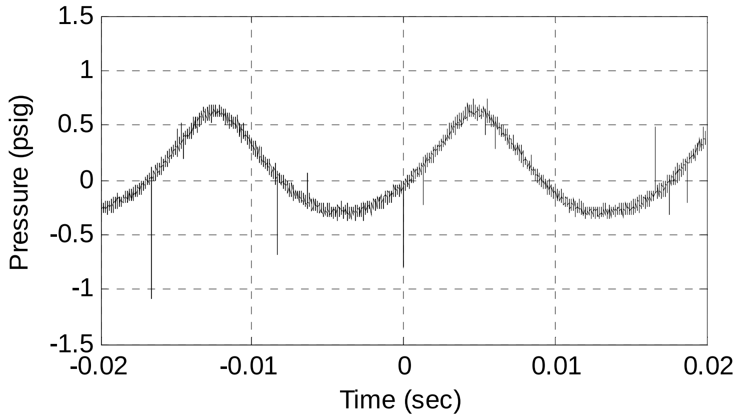

Figure 13: Pressure Measurement at 58.06 Hz

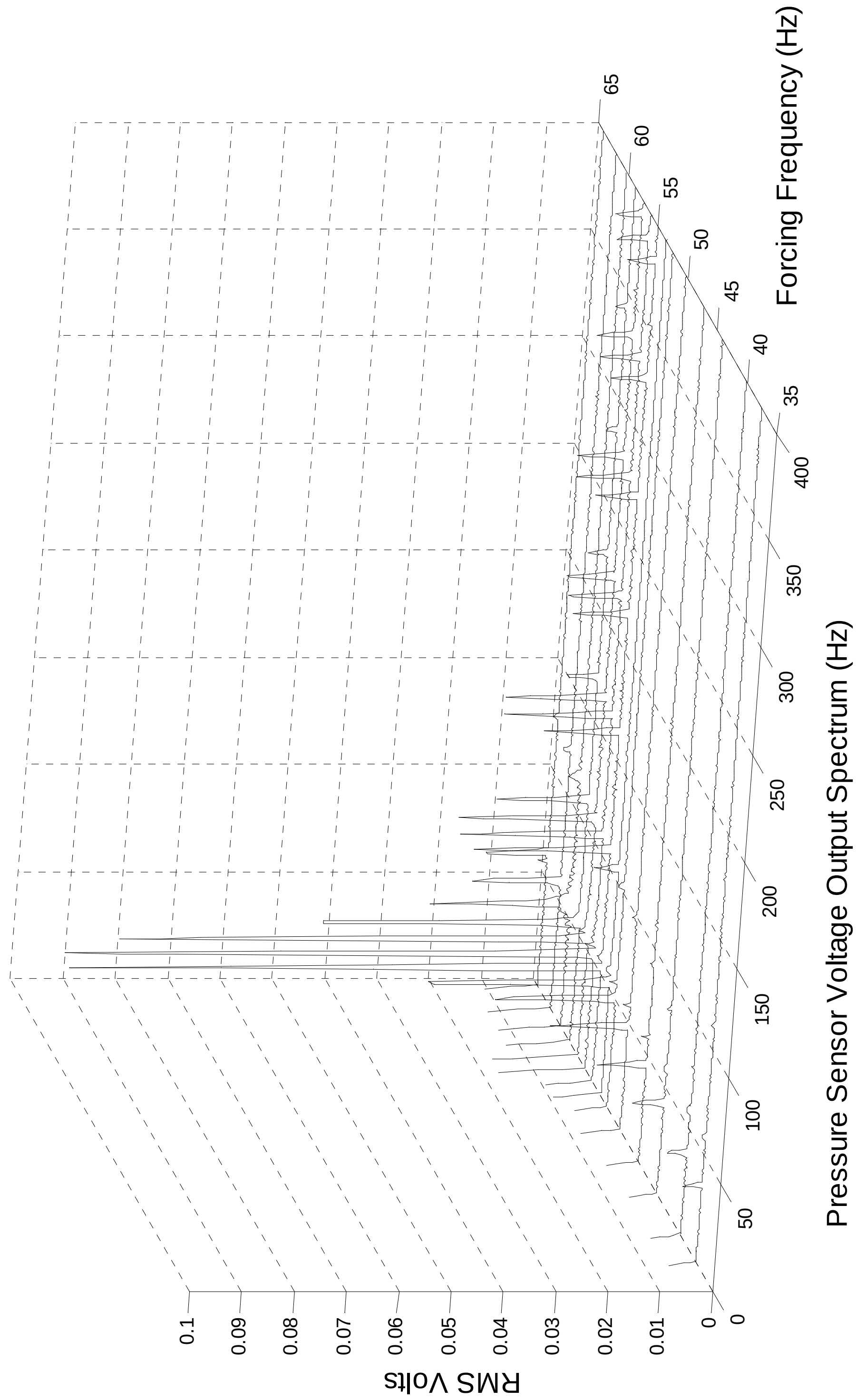

Figure 14: Pressure Spectrum Waterfall

3.3. Mean Pressure Shift

When the excitation frequency was near to the fundamental frequency of the closed tube, the mean pressure in the tube increased. This increase was measured by the water manometers. Interestingly the mean pressure increase differed between the middle and the end of the tube by approximately 40 percent. Figure 15 shows pressure data taken from the water manometers as the pistons forcing frequency varied.

As the input frequency grew and surpassed the resonance frequency the mean pressure in the tube fell. However, it did not fall down to a level which was present before the harmonic resonance; this 'hysteresis' effect can be shown by running the experiment from a high initial frequency to a low frequency. The build up of pressure is likely due to the fact that the pressure in the tube has built up previously from the shock interaction. Figure 16 demonstrates that it is the passing through the resonance that creates this 'permanent' pressure increase.

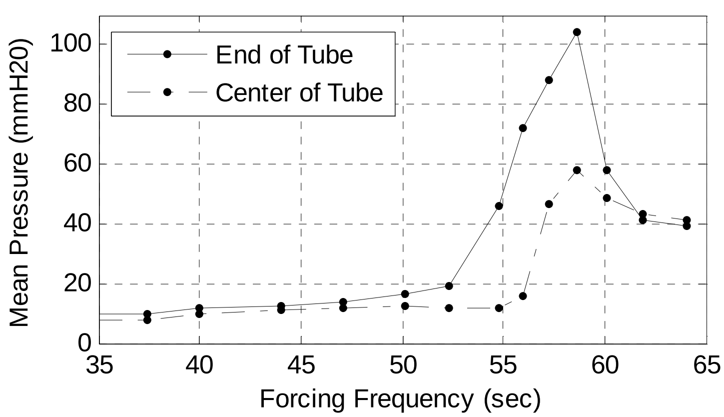

Figure 15: Mean Pressure Shift

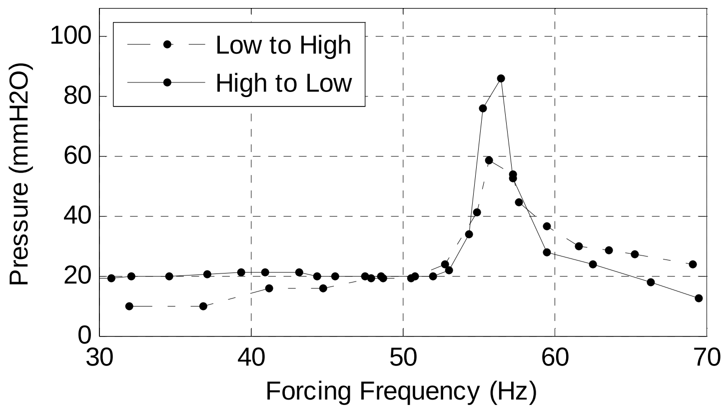

Figure 16: Mean Pressure Shift Hysteresis

4. Discussion of Results

4.1. Shock Waves and Spectral Analysis

In a linear analytical system, a piston driving a tube sinusoidally, at a given frequency, will only create sinusoidal pressure waveforms. When the linear system is driven near to the 1st mode of the tube, resonance will be achieved, and large amplitude sinusoidal waves will be present. Without damping infinitely large amplitudes are expected. At no point will higher harmonics be present; this makes the production of shock-like waveforms impossible.

In the experiment, the tube is driven by a piston which outputs nearly sinusoidal. However, the evidence of shock-like waves and generation of harmonics in the system is clear. Figure 12 shows a plot of the pressure waveform present when the tube is driven near to its fundamental frequency. When the tube is driven away from its fundamental frequency sinusoidal waveforms are present, as can be seen in Figure 11. This gives clear evidence that a linear analytical approach is not appropriate for this system when it is driven near to its fundamental frequency. A non-linear analytical approach is necessary to capture the critical details of the closed tube system.

Analysis done by Chester[5] shows a near exact analytical result to the waveforms recorded in the experiment. Comparing the waveforms in Figures 11-13 against the analytical plot shown in Figure 6 shows a noticeable relation. The work done by Chester[5] can very accurately predict the non-linear waveforms seen in a closed tube driven system.

In a rocket engine it is more difficult to prove that a non-linear model is needed. Interaction of the combustion and flow field causes a piston-like driving of the fluid. This interaction causes the system to respond similarly to the experiment and shock-like waveforms and multiple harmonics are generated. Several scientists[18-21] argue that these are separate harmonics that are all being driven independently, as it is difficult, or impossible, to measure which frequencies in the combustion processes are driving the flow. Assuming that these harmonics are independent allows the use of linear analytical models. However, these linear models fail to predict important characteristics of the rocket engine's performance such as the mean pressure shift in the motor when the shock-like waveforms are present.

Others[6,16-17] argue that these shock-like waveforms are consequences of non-linear interactions. The combustion processes can cause disturbances in one harmonic, and the energy from that harmonic will cascade to higher harmonics. This creates the shock-like waveforms. The experiment shows that it is not necessary that all the harmonics are being driven independently and that consequently a non-linear model is more appropriate.

4.2. Mean Pressure Shift and Variation across Tube

The mean pressure increase in the tube is a feature which current linear models are unable to predicted, as there is no mechanism in the analytics to allow the mean pressure to change. When the shock-like waves were present in the system, the mean pressure of the tube increased. This increase in mean pressure is due to the fact that the piston is doing non-linear pdV work on the fluid. This work enters the system in two ways. The first is to increase the amplitude of the waveforms, which thereby leads to the cascading of energy and the shock-like features. The second is to increase the mean pressure of the system. This energy is also expected to increase the mean temperature of the system as well, however, there was not an attempt made to measure this.

Figure 15 shows the plot of the mean pressure shift vs. forcing frequency. Two important features can be noticed. The first is the increase in the mean pressure and the frequency at which it meets its maximum. This maximum takes place at a higher frequency than expected with the calculation of the closed tubes fundamental harmonic. This is likely due to an increase in mean temperature which influences the speed of sound and harmonic frequencies. This hypothesis encourages more work to be done to measure the temperature in the tube to gain a better understanding of the conditions and speed of sound in the tube.

Secondly, the mean pressure increase was found to change within the length of the tube. This phenomenon is shown in the analytical work done by Flandro via a person correspondence and is shown to be the result of nonlinear pdV work done on the chamber gas by pressure coupling in the case of rocket flows and by the piston motion in the present case.

The mean pressure increase is a significant component in the design of a rocket combustion chamber. An increase in mean pressure can cause the catastrophic failure of the rockets engine. Understanding this phenomenon is critical for design and can only be done with the use of the non-linear analytical approach.

4.3. Recommended Alterations to Experiment

In the process of designing, building, and running the experiment several lessons have been learned. Interesting results have been uncovered and will lead to future research. Some changes and advancements are thereby suggested for future experimentation.

The experimental setup can be advanced with the use of digital manometers recording the mean pressure in the tube. This would allow a direct measurement of the pressures and reduce or eliminate any human error involved. Also, additional manometers could be placed along the length of the tube, gathering a more complete view of the change in mean pressure along the length of the tube.

It is evident in the analytics that a mean temperature increase should be present. It was initially decided to avoid measuring this change, as a small change in temperature may be difficult to measure. After operating the experiment it is clear that these measurements are more important than expected. Measuring a mean temperature shift will further increase the evidence that a non-linear model is necessary.

The closed tube was only driven shortly above its 1^{st} harmonic. Driving the tube at higher frequencies, up to and past its 2^{nd} mode should, according to the theory, produce similar shock-like features and mean pressure increase. It would also be interesting to see where the energy cascades to. What will the amplitude of the 1^{st} harmonic be when only the 2^{nd} mode is driven?

This experiment only dealt with the driving and measurement of longitudinal waves in a closed tube. In rocket combustion chambers tangential and radial modes appear along with the longitudinal modes. These other waves could be driven and measured with similar setups as the shown experiment.

The experiment was done with only one set of parameters. Addition experiments could be done by changing important parameters such as tube length, tube diameter, tube material, piston diameter, piston stroke and also utilizing different gas properties.

5. Conclusion

The experiment preformed was setup so that the pressure waveform and the mean pressure in the tube could be accurately measured. The results of the experiment show that there are clear non-linear aspects to a problem generally considered and treated to be linear. These non-linear aspects come in the form of shock-like structures with cascading of energy and mean pressure shifts, all of which are impossible to predict with traditional linear acoustic theory.

The pressure recordings are also similar to those seen in Chesters[5] analytical work where he shows the waveforms to be non-linear in nature. The mean pressure shift is shown in work by Flandro.[6,16-17] These analytical insights give light to the underlying physical mechanisms at work in the system and allow this work to be applied to the design of rocket chamber combustion instability analysis.

The shock-waves and spectra are similar in fashion to that seen in the shuttle SRB and JPL research motors. The mean pressure shift while the shock-like waves are present is also similar to those seen in solid rocket pressure readings. These results have real value in the area of rocket combustion instability where shock-like structures and mean pressure shifts are common in unstable rockets. Having a full understanding of the fundamental processes at work in a driven closed tube system are critical in understanding the complex events that occur in a rockets combustion chamber. The results shown here validate that the current non-linear analytical approach is the correct one.

References

References

[1]Saenger, R. A., “Periodic Shock Waves in Resonating Gas Columns,” Doctoral Dissertation, New York University, New York, NY, December 1958.

[2]Saenger, R. A. and Hudson, G. E., “Periodic Shock Waves in Resonating Gas Columns,” *The Journal of the Acoustical Society of America*, Vol. 32, No. 8, August 1960, pp. 961-970.

[3]Temkin, S., “Nonlinear Gas Oscillations in a Resonant Tube,” *The Physics of Fluids*, Vol. 11, No. 5, pp. 960-963.

[4]Betchov, R., ”Nonlinear Oscillations of a Column of Gas,” *The Physics of Fluids*, Vol. 1, No. 3, pp. 205-212.

[5]Chester, W., ”Resonant Oscillations in a Resonant Tube,” *The Journal of Fluid Mechanics*, Vol. 18, pp. 44-64.

[6]Flandro, G. A., Fischbach, S. R., Majdalani, J., and French, J. C., “Nonlinear Rocket Motor Stability Prediction: Limit Amplitude, Triggering, and Mean Pressure Shift,” *AIAA Paper* 2004-4054, July 2004.

[7]Sotter, J.G., Woodward, J. W., and Clayton, R.M., “Injector Response to Strong High-Frequency Pressure Oscillations,” *Journal of Spacecraft and Rockets*, Vol. 6, No. 4, 1969, pp. 504-506.

[8]Sotter, J.G. and C., R. M., “Monitoring the Combustion Process in Large Engines,” *Journal of Spacecraft and Rockets*, Vol. 4, No. 5, 1967, pp. 702-703.

[9]Clayton, R. M., “Experimental Measurements on Rotating Detonation-Like Combustion,” JPL, Technical Rept. 32-788, Pasadena, CA, August 1965.

[10]Clayton, R. M., Rogero, R. S., and Sotter, J. G., "An Experimental Description of Destructive Liquid Rocket Resonant Combustion," *AIAA Journal*, Vol. 6, No. 7, 1968, pp. 1252-1259.

[11]Flandro, G. A., "Vortex Driving Mechanisms in Oscillatory Rocket Flows," *AIAA Journal*, Vol. 2, No. 3, 1986, pp. 208-214.

[12]Bloomshield, F. S., "Stability Testing and Pulsing of Full Scale Tactical Engines, Parts I and II," *Naval Air Warfare Center*, 1996.

[13]Bloomshield, F. S., C. J. Bicker, et al. (eds.), "High Pressure Pulsed Firing Combustion Instability Investigations," *Proceedings of the 1996 JANNAF 33rd Combustion Meeting*, Montery, CA, Naval Postgraduate School, 1996.

[14]Bloomshield, F. S., J. E. Crump, et al., "Stability Testing of Full-Scale Tactical Engines," *Journal of Propulsion and Power*, Vol. 13, No. 3, 1997, pp.349-355.

[15]Harrje, D.T., and Reardon, F. H. (eds.), "Liquid Propellant Rocket Combustion Instability," *NASA SP-194,* 1972.

[16]Flandro, G. A., "Approximate Analysis of Nonlinear Instability with Shock Waves," *AIAA Paper 82-1220*, July 1982.

[17]Flandro, G. A., "Energy Balance Analysis of Nonlinear Combustion Instability," *Journal of Propulsion and Power*, Vol. 1, No. 3, 1985, pp. 210-221.

[18]Culick, F. E. C., "Acoustic Oscillations in Solid Propellant Rocket Chambers," *Acta Astronautica*, Vol. 12, No. 4, 1966, pp. 113-126.

[19]Culick, F. E. C., "The Stability of One-Dimensional Motions on a Rocket Motor," *Combustion Science and Technology*, Vol. 7, No. 4, 1973, pp. 165-175.

[20]Culick, F. E. C., "The Stability of Three-Dimensional Motions on a Rocket Motor," *Combustion Science and Technology*, Vol. 10, No. 3, 1974, pp. 109-124.

[21]Hart, R. W., and McClure, F. T., "Theory of Acoustic Instability in Solid Propellant Rocket Combustion," *Tenth Symposium (International) on Combustion,* 1964, pp. 1047-1066.

Appendix

Appendix

A.1 F-1 decibel calculations

$$20 * \log \frac{4826330 Pa}{.00002 Pa} = 227.65 dB$$

A.2 Speed of Sound and Fundamental Harmonic Calculations

The speed of sound, *a*, of the air in the tube was calculated using the equation,

$$a = \sqrt{\gamma \cdot R \cdot T}$$

Where

$$\gamma = 1.4$$
$$R = 1716 \frac{ft \cdot lbf}{slug \cdot {}^{O}R}$$
$$T = 67 \pm 5^{O} F$$

This yields a speed of sound of 1124.84 ft/sec (+/- 5 ft/sec). In the experiment, the temperature of the air in the tube is not necessarily a constant; therefore more variation in the speed of sound in the tube is expected.

The fundamental harmonic of the tube was calculated by using the equation,

$$h = \frac{a}{2 * L}$$

Where

$$L = 10.0 \pm .01 ft$$

This yields a fundamental harmonic of 56.2 Hz (+/- .3 Hz).

A.3 Additional Experimental Setup Photos

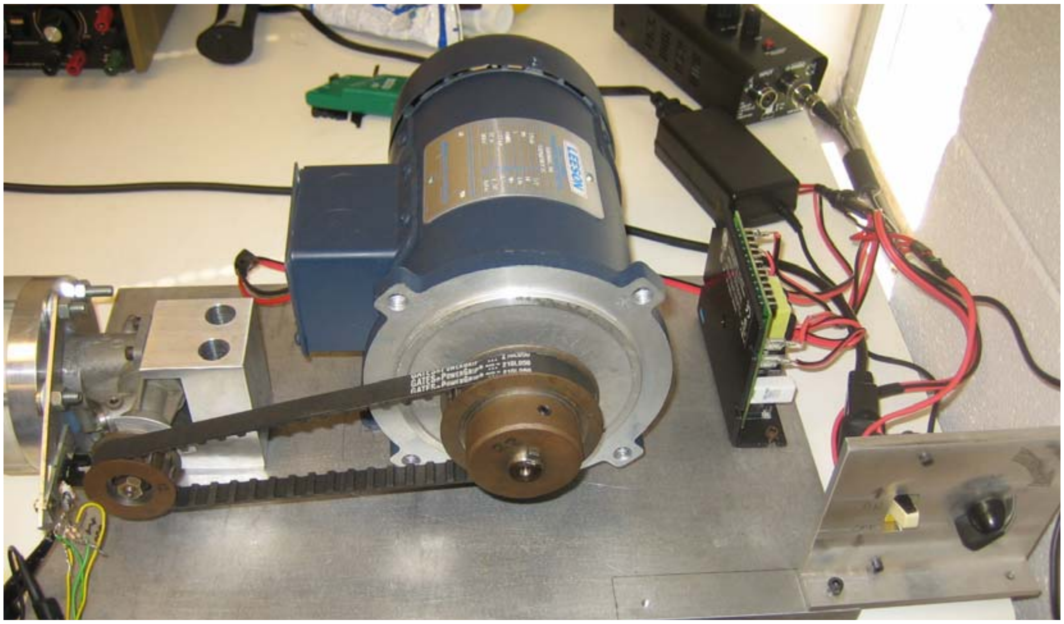

Figure 17: DC Motor with Piston

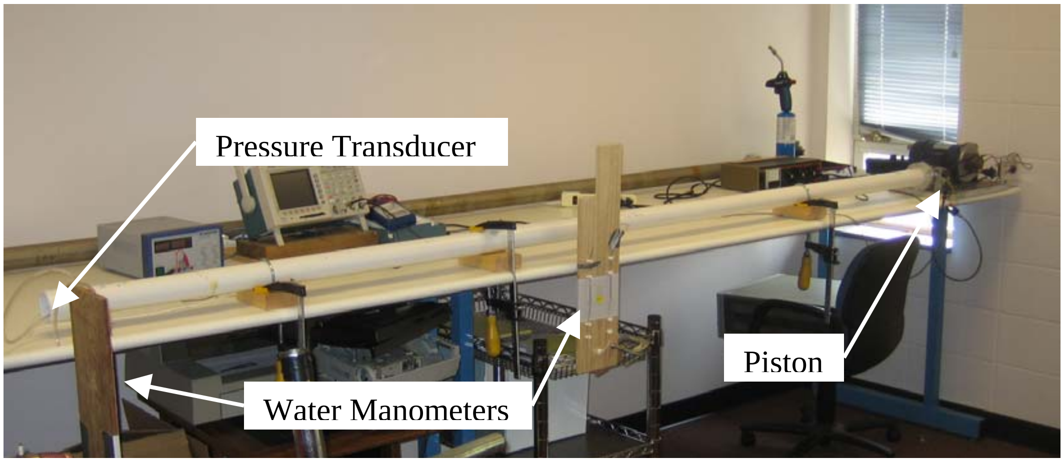

Figure 18: Location of Pressure Sensors in Photograph

A.4 Additional Waveform Plots

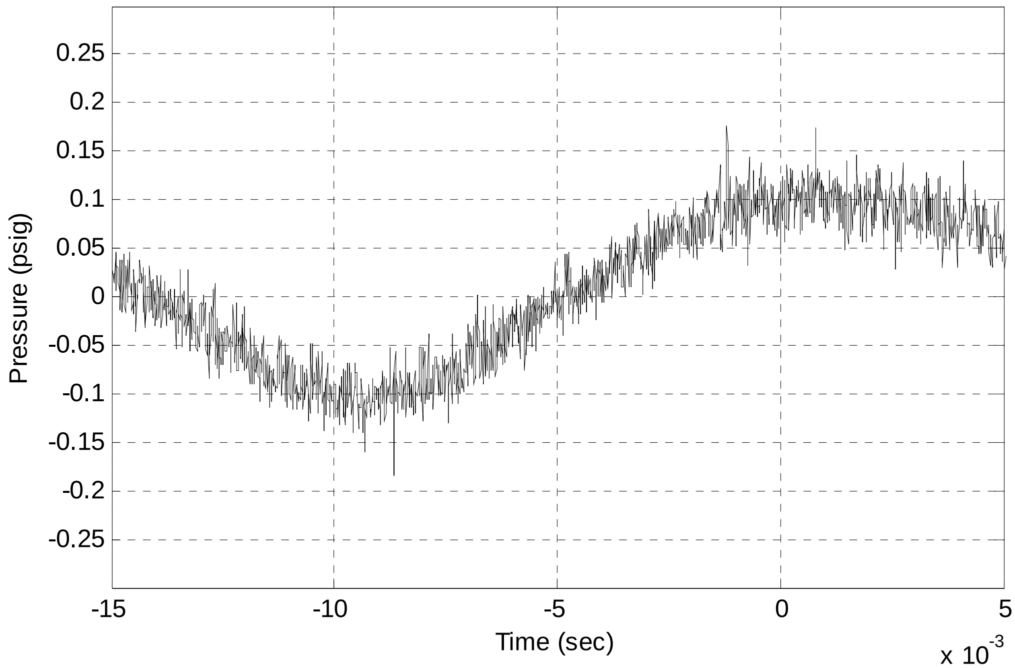

Figure 19: Expanded Pressure Measurement at 43.43 Hz

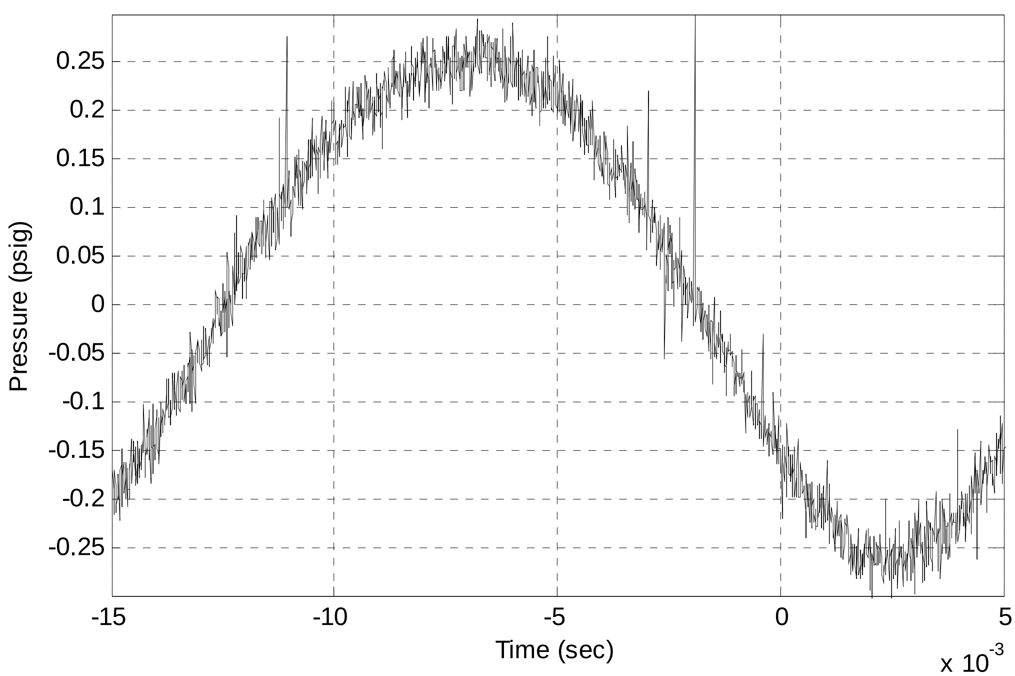

Figure 20: Expanded Pressure Measurement at 47.72 Hz

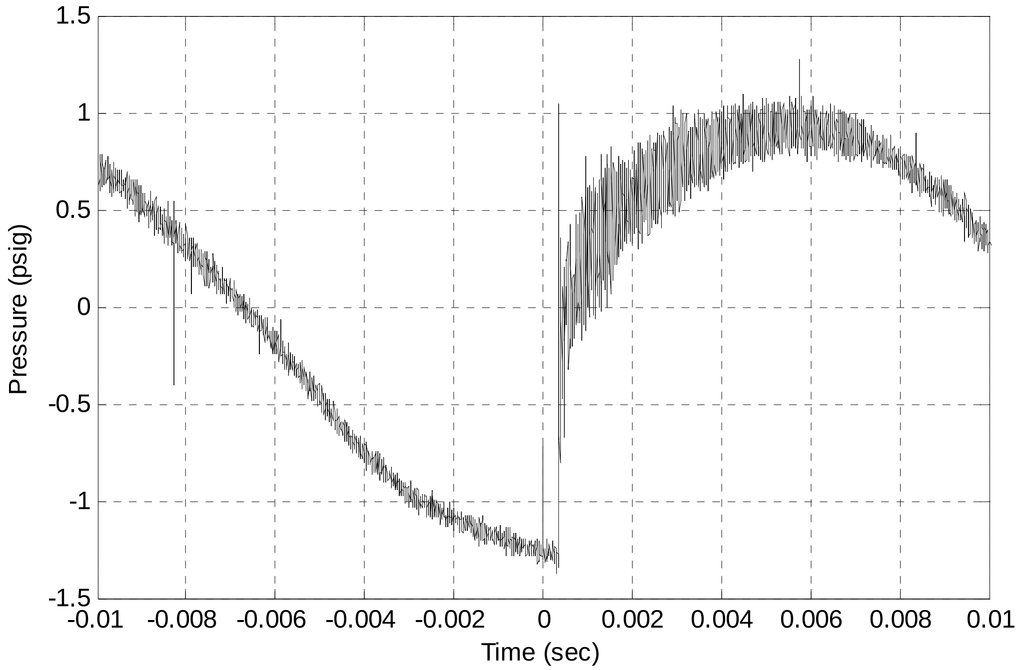

Figure 21: Expanded Pressure Measurement at 54.99 Hz

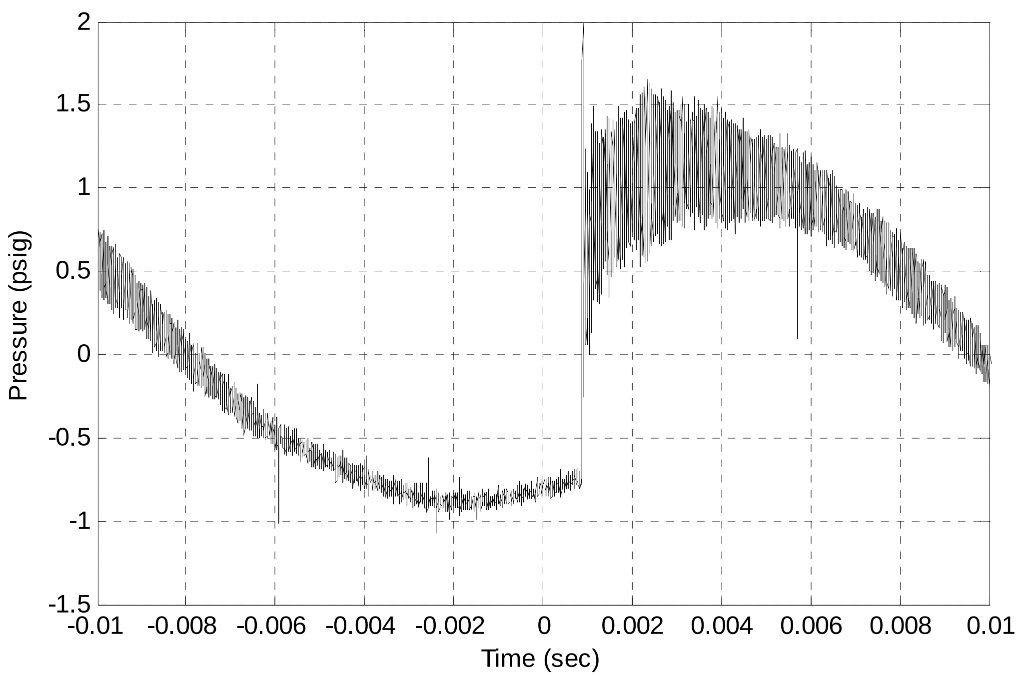

Figure 22: Expanded Pressure Measurement at 56.11 Hz

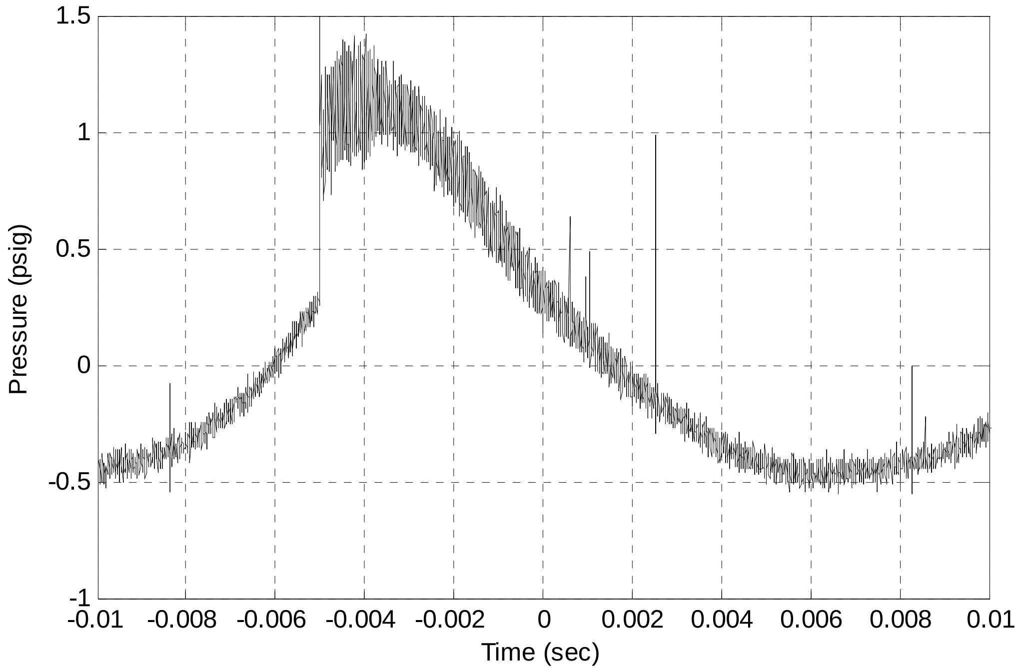

Figure 23: Expanded Pressure Measurement at 57.11 Hz

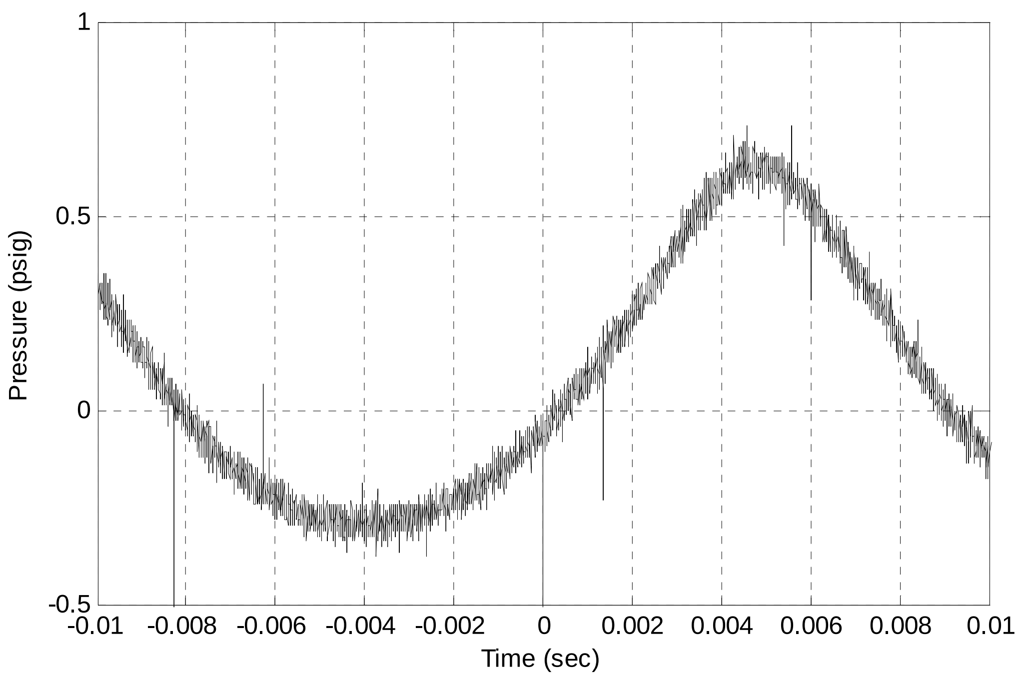

Figure 24: Expanded Pressure Measurement at 58.06 Hz

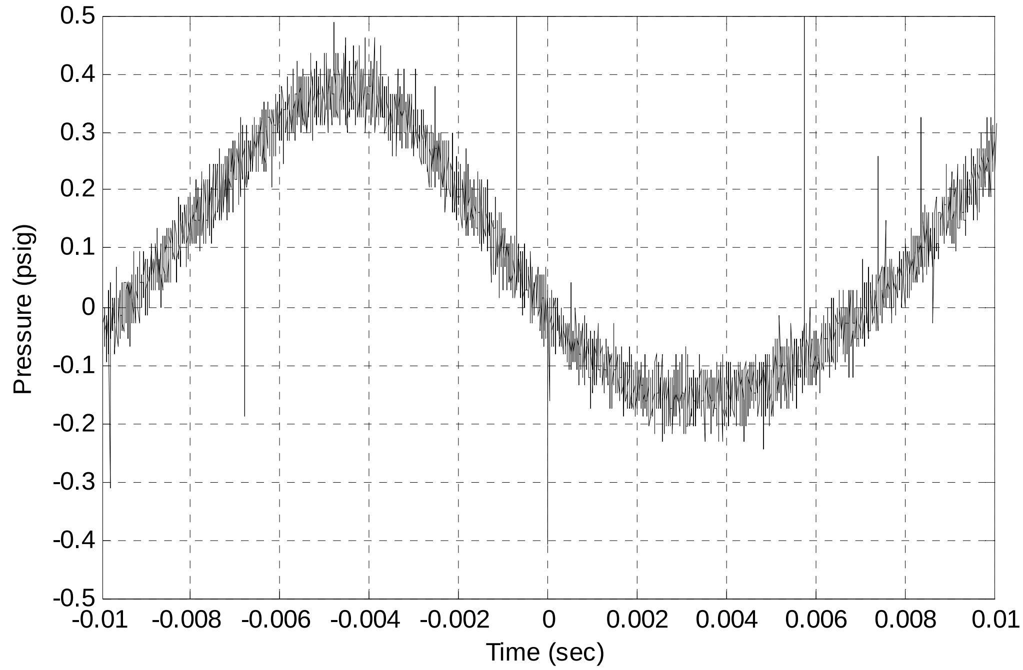

Figure 25: Expanded Pressure Measurement at 59.58 Hz

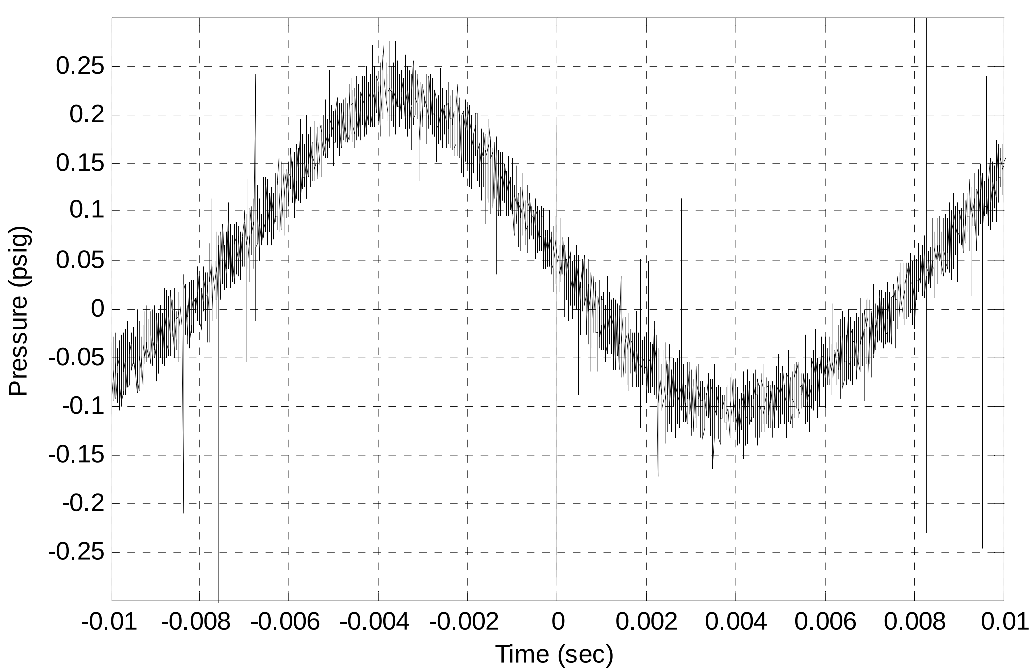

Figure 26: Expanded Pressure Measurement at 63.23 Hz

A.5 Sawtooth Wave Harmonics

The shock-like waveforms seen when the closed tube is excited near to its fundamental frequency is similar to a sawtooth wave. Figure 27 shows the modal amplitudes of the sawtooth wave when decomposed using Fourier series. These harmonics bear a striking resemblance to the spectra seen in the closed tube.

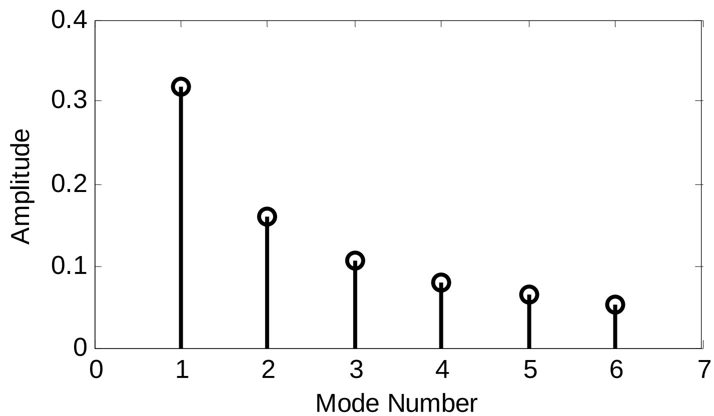

Figure 27: Sawtooth Fourier Series Modal Amplitude

A.6. Chester's Analytic Results

The plot shown in Figure 6 depicts the analytical results from Chester.[5] The value r is given by the equation:

$$r = \frac{\pi a_o \tan\left(\omega L / a_o \right)}{(\gamma + 1)\omega L \varepsilon^{1/2}}$$

Where

$$a_o = Speed\ of\ Sound$$
$$\omega = Driving\ Frequency$$
$$L = Length\ of\ Tube$$
$$\gamma = Ratio\ of\ Specific\ heats, \frac{c_p}{c_v}$$
$$\varepsilon = \frac{4\ell}{(\gamma+1)L\left|\cos(\omega L / a_o)\right|}$$
$$\ell = Piston\ Stroke\ Length$$

The output function is given as a function of r. Split into three categories, if $|r| > 1$ then,

$$f = \varepsilon^{1/2}\left[\frac{2r}{\pi} \pm \left(b^2 + \cos^2\tau\right)^{1/2}\right]$$
$$|r| = \left(1+b^2\right)^{1/2} E\left\{\left(1+b^2\right)^{1/2}\right\}$$

Where E is a complete elliptic integral of the second kind and

$$\tau = \frac{\omega t}{2} - \frac{j\pi}{4}$$
$$b = \sqrt{\frac{1}{p^2} - 1}$$

Where p is an adjustable parameter. If $|r| = 1$, then,

$$f = \varepsilon^{1/2}\left[\frac{2}{\pi} \pm \cos\tau\right]$$

This yields a rectified sine wave that is displaced to make the mean value equal to zero.

If $|r| < 1$, then,

$$f = \varepsilon^{1/2}\left[\frac{2r}{\pi} + \cos\tau\right]$$

Thereby producing one discontinuity in each complete period.

Vita

Eric James Jacob was born in West Allis, WI on July 3rd, 1982. After finishing high school in 2000 he attended The Milwaukee School of Engineering of Milwaukee, WI. In the spring of 2004 he received a Bachelors of Science degree in Mechanical Engineering with a minor in physics.

In August of 2004 he began graduate studies in the Mechanical, Aerospace and Biomedical Engineering department at the University of Tennessee Space Institute. From 2004 to 2006 Eric designed, built and ran experiments on nonlinear acoustics under the guidance of Dr. Flandro. He will be graduating with a Master of Science degree in Aerospace Engineering in the fall of 2006. He plans on continuing his doctoral education at the University of Tennessee Space Institute.